Journal of Materials Chemistry A

Accepted Manuscript

ROYAL SOCIETY OF CHEMISTRY

www.rsc.org/materialsA

Journal Name

RSCPublishing

ARTICLE

Ordered Mesoporous Silica/Polyvinylidene Fluoride Composite Membranes with Three-Dimensional Interpenetrating Structures for Effective Removal of Water Contaminants

Cite this: DOI: 10.1039/xoxxoooooox

Received ooth January 2012,
Accepted ooth January 2012

DOI: 10.1039/xoxxoooooox

www.rsc.org/

Jianwei Fan,[a] Dandan Li,[a] Wei Teng,[a] Jianping Yang,[a] Yong Liu,[b] Liangliang Liu,[b] Ahmed A. Elzatahry,[d] Abdulaziz Alghamdi,[e] Yonghui Deng,*[b,c] Guangming Li,[a] Wei-xian Zhang,[a] and Dongyuan Zhao[b]

A facile one-step immersion co-precipitation method has been developed to fabricate an inorganic-organic composite membrane with three-dimensionally (3D) interpenetrating porous structures via incorporating ordered mesoporous silica (OMS) into polyvinylidene fluoride (PVDF). The composite membranes possess high surface area, excellent hydrophilicity and ultrahigh water fluxing capability (224.5 L m^{-2} h^{-1}). It shows an excellent dynamic adsorption capacity (14.5 mg g^{-1}) for methylene blue, which is ~ 9.7 times higher than that of the pure PVDF membranes. Moreover, the composite membrane containing amino-functionalized OMS exhibits good adsorption capacity (1.5 mg g^{-1}) for Cu (II) ions, thanks to the numerous amino groups in the mesopore walls. Importantly, the composite membranes can be easily regenerated, retaining the adsorption performance. Our findings open up the possibility for the mass fabrication of functional porous membranes for continuous and scalable water treatment.

Introduction

Ordered mesoporous silica (OMS) materials have attracted a great deal of research attention for their wide potential applications as adsorbents. The outstanding features (high surface areas, large pore volumes, uniform and tunable pore sizes) endow such an adsorbent to have high adsorption capacity with fast adsorption kinetics for a wide size-range of guest molecules.[1] In addition, the mesopore surfaces can be easily modified or functionalized with particular functional moieties, enabling the possibility of specific binding, enrichment, and separation of various water contaminants.[2] However, broad usesof the OMS materials in adsorption technology still remaingreat challenges. In general, OMS materials are available mainly in powdered form, which are difficult to be employed in any flowing streams for their high energy requiring for separation and regeneration process.[3] Although there are few recent literature reports on synthesis of OMS materials in the form of thin films or monoliths, they are also quite disadvantageous for large-scale practical processes due to their low mechanical strength.[4] Therefore, it is fairly demanding to explore new approaches to expand the applicability of OMS materials in adsorption and separation process for water decontamination.

In recent decades, there have been considerable interests in developing advanced methods for water decontamination, such as adsorption using porous materials,[1a, 5]catalytic redox system using various catalysts,[6] and separation process based on organic polymer membrane filtration. By contrast, the polymeric membrane separation process exhibits outstanding advantages in water treatment owing to their low energy consumption and easy recyclability compared with other methods.[7] However, conventional polymeric membranes such as polyvinylidene fluoride (PVDF),[8]polysulphone (PS),[9] and polytetrafluoro-ethylene (PTFE)[10] membranes mostly separate the contaminants based on size exclusion effect rather than adsorption process,[11, 12] which results in poor decontamination performance. Therefore, it is of great significance to assemble OMS materials into traditional polymeric membranes to combine their advantages and overcome their respective drawbacks in water decontamination.

In recent years, PVDF has become one of the most commonly used membrane materials for water treatment due to its outstanding properties such as high mechanical strength, thermal stability, and excellent chemical resistance.[8a] To date, the immersion precipitation process is the most widely used method to fabricate PVDF membranes owing to its simplicity and flexible production scales.[13] As the PVDF membrane is hydrophobic in nature and susceptible to fouling, hence many studies have been focused on hydrophilicity modification by blending hydrophilic inorganic particles such as Al_2O_3,[14] TiO_2,[15] and SiO_2[16] in polymer solutions during the immersion precipitation process. The obtained inorganic/polymeric composite membranes present an interesting approach for selectively modifying the polymeric membranes without affecting the fabrication mechanism. To the best of our knowledge, investigations on fabricating such a composite membrane by assembly of OMS materials and PVDF have rarely been reported. It is expected that,

Journal Name

RSCPublishing

ARTICLE

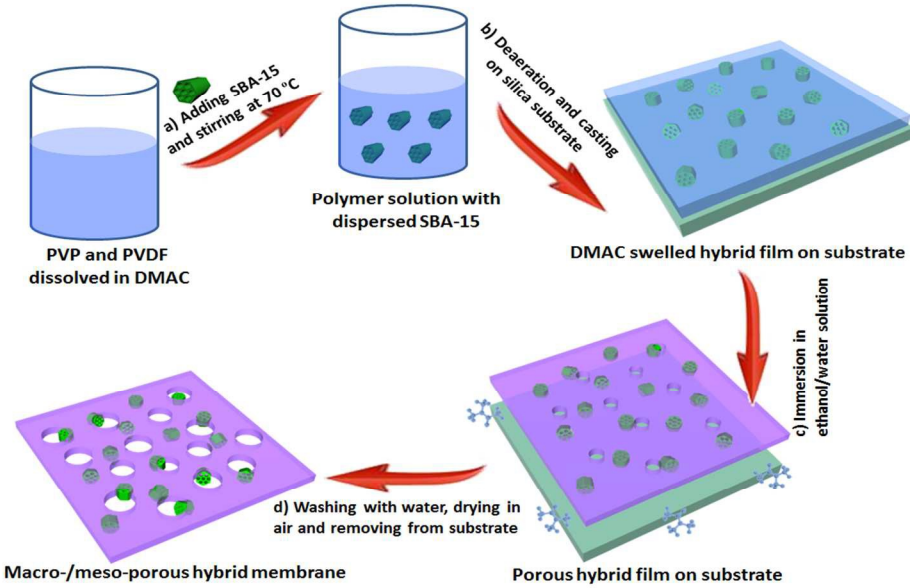

Scheme 1. Illustration of the fabrication process of mesoporous silica/polyvinylidene fluoride (OMS/PVDF) hybrid membrane via the one-step immersion co-precipitation method. (a) preparation of homogeneous casting solution by dispersing SBA-15 in the dimethylacetamide solution containing PVDF and polyvinylpyrrolidone (PVP), followed with stirring for 24 h at 70 °C; (b) the membrane coating process by casting the obtained solution onto a glass substrate uniformly after complete deaeration; (c) The phase separation process by immersing the glass substrate with the casting solution in a coagulation bath filled with deionized water and ethanol (1:1 by volume) after exposure in air for 40 s; (d) washing the composite film using deionized water, drying at room temperature and finally removing from the substrate, resulting in flexible macro-/meso- porous hybrid membrane.

owing to the outstanding mesoporous structures and high surface areas of OMS, the OMS/PVDF composite membranes thus can effectively interact with water contaminants not only through the external membrane surfaces, but also *via* active adsorption sites located on the pore walls of OMS materials.

Both dye molecules and heavy metal ions are common water pollutants, which are toxic both to aquatic life and humans even in very low concentrations. Conventional methods for the removal of dye molecules, such as biological oxidation and chemical precipitation, and common methods for the removal of heavy metals, such as chemical precipitation, reverse osmosis, and coagulation/co-precipitation, are effective and economic only in the case where the solute concentrations of contaminants are relatively high. As adsorption is known as one of best methods for the removal of low concentrations of contaminants, the OMS/PVDF composite membranes may have great potential in the removal of both low-concentration dye molecules and heavy metals.

Herein, we report a versatile and industrially compatible one-step immersion co-precipitation strategy for assembly of OMS materials and PVDF into composite membranes with enormous active adsorption sites for water contaminants. The membrane with ~ 3 wt % OMS content (OMS/PVDF-3) exhibits strong hydrophilicity and ultrahigh water flux (224.5 L m^{-2} h^{-1}). When employed for dynamic adsorption tests, the OMS/PVDF-3 composite membrane shows excellent dynamic adsorption capacity (14.5 mg g^{-1}) for methylene blue, almost 9.7 times higher than that of the pure PVDF membrane. The composite membrane containing ~ 3 wt % of amino-group functionalized OMS (OMS-NH_2) shows good adsorption capacity (1.5 mg g^{-1}) for Cu (II) ions, while the OMS/PVDF-3 shows almost no adsorption for Cu (II) ions due to the lack of active adsorption sites. Furthermore, the composite membranes show highly stable regeneration performances. By combining the advantages of high capacity of OMS materials and the capability of polymeric membranes, such OMS/PVDF composite membranes may have a great potential in flowing water decontamination.

Experimental section

Chemicals

Triblock copolymer poly(ethylene oxide)-b-poly(propyleneoxide)- b-poly(ethylene oxide) Pluronic P123 ($EO_{20}PO_{70}EO_{20}$,with an average Mw of 5800), tetraethoxysilane (TEOS), ethanol, 3-aminopropyltriethoxysilane (APTES), hydrochloric acid, polyvinylidene fluoride (PVDF), polyvinylpyrrolidone (PVP, K30), dimethylacetamide (DMAC), silicon oxide (SiO_2), methylene blue (MB), and copper (II) nitrate trihydrate ($Cu(NO_3)_2 \cdot 3H_2O$) were purchased from Sigma-Aldrich. All chemicals were used as received without further purification. Deionized water was used for all experiments. Anhydrous

$FeCl_3$, trisodium citrate, sodium acetate, tetraethyl orthosilicate (TEOS), Resorcinol, formaldehyde, $HAuCl_4 \cdot 3H_2O$, ethanol, ethylene glycol, concentrated ammonia solution (28 wt %) are of analytical grade (Shanghai Chemical Corp.). Cetyltrimethyl ammonium bromide (CTAB) and *tert*-Butyl hydroperoxide (70 wt % in water) was supplied by Aldrich-sigma. Styrene was purified by filtrating through Al_2O_3 column. All other chemicals were used as received. Deionized water was used for all experiments.

Synthesis of ordered mesoporous silica and amino-group functionalized ordered mesoporous silica. The pristine ordered mesoporous silica (OMS) was synthesized by using a triblock copolymer Pluronic P123 as the structure-directing reagent and TEOS as a silica precursor according to previous report.[17] Amino-functionalized ordered mesoporous silica (OMS-NH_2) was prepared by post synthetic modification method.[18] Prior to surface functionalization, the prepared OMS was activated overnight at 110 °C under vacuum. Then 1.5 g of the activated OMS was dispersed in 150 mL of anhydrous toluene with stirring for 0.5 h. Subsequently, 1.2 g of 3-aminopropyltriethoxysilane (APTES) was added, and the mixture was refluxed with stirring at 80 °C for 16 h. The solid was then filtered, washed several times with toluene and ethanol, and finally dried at 60 °C in vacuum for 12 h.

Fabrication of membranes. The ordered mesoporous silica/polyvinylidene fluoride (OMS/PVDF) composite membranes were fabricated by a one-step immersion co-precipitation method. Polyvinylidene fluoride (PVDF), polyvinylpyrrolidone (PVP) and the prepared ordered mesoporous silica (OMS) were primarily dried at 110 °C for 4 h to remove residual water. PVDF (17 wt %) and PVP (4 wt %) were uniformly dissolved in dimethylacetamide (DMAC, 79 wt %) by stirring at 250 rpm for 12 h under 70 °C. Then different amounts of the prepared OMS (1-5 wt % based on the casting solution) were added into the polymer solution with DMAC as the thinner (31 wt % based on the casting solution) by vigorously stirring for 24 h to give a homogeneous casting solution. To prepare homogeneous and defect-free membranes, the casting solutions were degassed in vacuum for 12 h. The resultant solutions were cast uniformly onto a glass substrate with a JFA-□ film applicator, and then the glass substrate was immersed into the coagulation bath containing deionized water and ethanol with a volume ratio of 1:1. After exposure to air for 40 s, the formed membrane was peeled off from the glass substrate and immersed in the coagulation bath for 24 h. Finally, the obtained membrane was thoroughly washed with deionized water to remove residual solvent and dried at room temperature. The obtained composite membranes with different contents of the OMS (1, 2, 3, 4, 5 wt % based on the casting solution weight) are donated as OMS/PVDF-1, 2, 3, 4, and 5, respectively. The composite membranes using OMS-NH_2 and commercial SiO_2 as fillers (3 wt % based on the casting solution) were also prepared according to the same method mentioned above, which are donated as OMS-NH_2/PVDF-3 and SiO_2/PVDF-3, respectively. For comparison, neat PVDF membrane without inorganic fillers was also prepared.

Measurements and characterization

Small-angle X-ray scattering. Small-angle X-ray scattering (SAXS) data of the mesoporous silica were collected on a Nanostar U small-angle X-ray scattering system (Bruker, Germany)using Cu Kα radiation at 40 kV and 35 mA. N_2 sorption isotherms were measured on a Micromeritics Model Tristar 3020 analyzer at 77 K. Before the measurements, the inorganic samples and membranes were degassed at 180 and 100 °C for 8 h, respectively. The surface areas (S_{BET}) were calculated based on the Brunauer–Emmet–Teller (BET) method. Scanning electron microscopy (SEM) imageswere collected on a Hitachi Model S-4800 field emission scanning electron microscope (Japan). The membrane samples were pretreated with gold-spraying, and the inorganic samples were directly used for the observation without any treatment. Static water contact angles of the membranes were recorded on an OCA20 contact angle measurement (Datephysics, Germany). Fourier transform infrared (FTIR) spectra were collected on Nicolet 5700 Fourier spectrophotometer. The C, H, and N contents were measured on a Vario EL III elemental analyzer (Germany). Water flux of the membrane samples were measured by a filtration device with N_2 cylinder providing the pressure. The membrane was previously compacted for 30 min at 0.15 MPa to get a steady flux, then the flux was recorded at 0.1 MPa every 5 min. at least 3 readings were collected to obtain an average value.

Dynamic adsorption of methylene blue (MB). The dynamic adsorption tests for MB by the obtained membranes were carried out on the experimental device as shown in Figure 1A. The experimental device was assembled by a feed container, a pump, a membrane module, and an effluent container. Four layers of stacked membranes were fixed in the membrane module, and the effective radius of which was 2.2 cm. During the dynamic adsorption tests, MB solution with an initial concentration of 5.0 mg L^{-1} was continuously pumped to filter through the membrane module at a flow rate of 98.7 L m^{-2} h^{-1}. The pH value of the MB feed solution was kept at 7.4 using the phosphate buffered saline (PBS) solution. Effluents from the outlet were consecutively collected at intervals of 5 min and analyzed using a spectrophotometer at 665 nm.

Regeneration of the membranes. Regeneration stability of the membranes was carried out by a continuous adsorption/desorption test using the same experimental device. For the membrane regeneration, a mixture solution of hydrochloric acid (0.5 mg L-1) and ethanol (1/1 by volume) was used as the eluent. After the permeation with 175 mL of MB feed solution, 100 mL of the prepared eluent were sequentially passed through the membrane module at the same flow rate (98.7 L m^{-2} h^{-1}) to elute the MB molecules adsorbed on the membranes. Then, 25 mL of PBS solution (pH = 7.4) was passed through the membrane module to wash out the ethanol and hydrochloric acid residues. Effluents from the outlet were consecutively collected at intervals of 5 min and analyzed using a spectrophotometer at 665 nm. The cycle was repeated for nine consecutive runs.

Dynamic adsorption of Cu (II) ions. The dynamic adsorption tests for Cu (II) ions by the membranes were carried out on the same experimental device as shown in Figure 1A. Cu (II) ion solution with an initial concentration of 2.0 mg L^{-1} was continuously pumped to filter through the membrane module at a flow rate of 39.4 L m^{-2} h^{-1}, which was composed of five layers of stacked membranes. The pH value of the feed solution was kept at 6.2 by using sodium hydroxide solution as the pH regulator. Effluents were consecutively collected at intervals of 5 min and analyzed through an inductively coupled plasma emission spectrometer (Agilent-720-ES). Regeneration tests of the membranes after the dynamic adsorption of Cu (II) ions were carried out by a continuous adsorption/desorption test using the same experimental device. The ethylene diamine tetraacetic acid (EDTA) disodium salt solution (0.5 mg L^{-1}) was used as the eluent. After the dynamic adsorption of 50 mL of Cu (II) solution, 20 mL of EDTA disodium salt solution followed with 10 mL of deionized water were sequentially passed through the membranes at a flow rate of 39.4 L m^{-2} $h^{-1}$to elute the Cu (II) ions and then wash out EDTA residues. The cycle was repeated for five consecutive runs. For each recycling, effluents were collected by allowing 50 mL of Cu (II) solution to

pass through the membranes and analyzed through the inductively coupled plasma emission spectrometer (Agilent-720-ES).

Results and Discussion

Small-angle X-ray scattering (SAXS) patterns of the as-synthesized OMS and OMS-NH_2 both show three well-resolved scattering peaks assigned to the 100, 110, and 200 reflections of space group *p6mm*(Figure S1), suggesting a highly ordered 2-D hexagonal mesostructure. Scanning electron microscopy (SEM) observation shows that the dimensions of the prepared OMS are 5 - 6.5 μm in length and ~ 2 μm in diameter (Figure S2 A), and the wheat-like morphology of the pristine OMS is well preserved in the OMS-NH_2 obtained after modification with 3-aminopropyltriethoxysilane (Figure S2 A, B). In addition, OMS-NH_2 has almost the same size as that of the pristine OMS and an N content of 1.2 wt% according to element analysis. The commercial SiO_2 powder consists of irregular nonporous nanoparticles of different sizes (Figure S2 C). N_2 sorption isotherms (Figure S2 D) of the pristine OMS and the OMS-NH_2 both show type-IV curves with H1-type hysteresis loops, indicating the existence of uniform channel-like mesopores. Compared with the pristine OMS, the OMS-NH_2 has lower absorption volume (0.48 $cm^3\ g^{-1}$) and surface area (367 m^2g^{-1}) (Table S1). The commercial SiO_2 has the lowest surface area (51 m^2g^{-1}) among the three kinds of inorganic fillers.

The fabrication processes of OMS/PVDF membranes are illustrated in Scheme 1. First, desired amount of OMS (1 ~ 5 wt % with respect to PVDF) was added into the mixed solution of PVDF, dimethylacetamide (DMAC), and polyvinylpyrrolidone (PVP) (Scheme 1 a). The obtained solution was stirred for 24 h at 70 °C to form a homogeneous casting solution (Scheme 1 b). After deaeration, the solution was cast uniformly onto a glass substrate (Scheme 1 c) and immersed in a coagulation bath filled with deionized water and ethanol (1:1 by volume) after exposure in air for 40 s. Upon immersion into the coagulation bath, water and ethanol (non-solvent) diffused into the casting solution, whereas DMAC (solvent) diffused into the bath. The exchange of solvent and non-solvent disturbed the solution system equilibrium and induced polymer precipitation (Scheme 1d).[19] Meanwhile, PVP in the casting solution was dissolved in the coagulation bath, which enhanced the phase separation and facilitated the formation of macro-pores in the obtained membrane. Finally, the membrane was washed with deionized water and dried at room temperature. For comparison, neat PVDF membrane and composite membranes using OMS-NH_2 and commercial solid SiO_2 nanoparticles as inorganic fillers were also prepared, respectively.

The pure PVDF membrane (Figure S3 A) and the OMS/PVDF-3 composite membrane (Figure S3B) both have continuous and defect-free morphology. SEM images of the top surface (Figure 1) and cross-section (Figure 2) show that all the obtained membranes exhibit typical spongy-like cross-section macroporous structures linked with a dense skin layer on the top surface, suggesting that the addition of the OMS has little effect on the formation process of the membrane. However, some slight differences can be seen between the pure PVDF membrane and the OMS/PVDF membranes. Top surface morphology of the pure PVDF membrane shows that macropores (0.3 – 0.5 μm) are uniformly distributed on the surface(Figure 1 A). With the addition of OMS (≤ 3 wt %), the pore sizes on the surface of the obtained membranes decrease slightly (0.1 – 0.25 μm) (Figure 1B, C, D).However, when the addition of OMS further increases (> 3 wt %), the top surfaces become coarse gradually, resulting in denser nodular-like membrane surfaces with large area of nonporous sections (Figure 1E, F). Generally, the decrease of surface pore sizes at low OMS additions is attributed to the increase of dope viscosity, which is unfavorable for the exchange of solvent and non-solvent during the phase separation process.[20] Consequently, precipitation rate of the polymer slows down, leading to dense surfaces with smaller pores. However, when the content of OMS in the casting solution is too high (> 3 wt %), the hydrophilic OMS tend to agglomerate with each other, resulting in dense membrane surfaces with unevenly distributed suppressed pores.

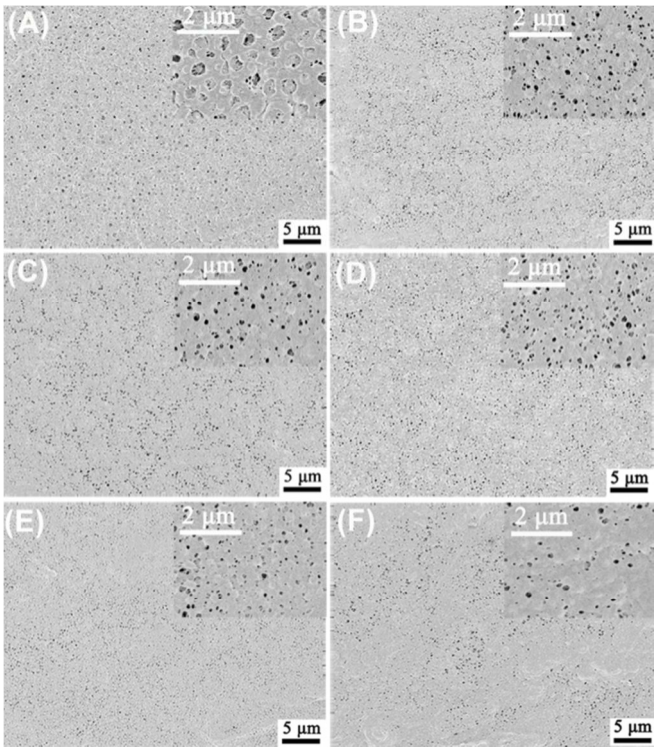

Figure 1. The SEM images taken along the top surface of the membranes with different adding amounts of the OMS: A) 0 wt %, B) 1 wt %, C) 2 wt %, D) 3 wt %, E) 4 wt %, and F) 5 wt %. All the weight percentages are based on the weight of the casting solution. The insets are the corresponding enlarged images.

The cross-section SEM image of the pure PVDF membrane (Figure 2 A) exhibits a typical spongy-like structure with homogenous and interpenetrating macropores. With the addition of OMS, the cross-section of the obtained membranes becomes more compact, similar with their top surface morphologies. At a low OMS addition (≤ 3 wt %), wheat-like OMS particles (marked by white arrows) are homogeneously distributed within the polymer networks (Figure 2B, D). Within the membranes, interpenetrating macropores resulted from the polymer networks are interconnected with the mesopore channels of the OMS, which can simultaneously increase the surface areas and permeation performance of the obtained membranes. However, further increasing the OMS addition could induces agglomeration (Figure 2E, F) of the hydrophilic OMS, which causes blockage of macropores in the obtained membranes, thus leading to compact and non-interpenetrating cross-section structures (see insets in Figure 2 E, F). To obtained interior information of the composite membranes, OMS/PVDF-3, as a typical sample, was submitted to ultrathin microtomming for TEM observations. The TEM images indicate that SBA-15 particles are well mixed with PVDF (Figure S4a), and the pore channels can be clearly visible, implying a well-controlled blending process of SBA-15 and PVDF (Figure S4b).

Based on the experiment results, the porosity of the pure PVDF is ~ 65.0%, which is smaller than that of the composite membranes. As the OMS content increases from 0 to 5 wt %, the porosity of the composite membranes increases slowly from 69.3% to 74.3% (Table S2), indicating that the addition of OMS has little effect on the porosities of the prepared composite membranes. Static water contact angles of the membranes were measured to study the effect of OMS contents on the surface hydrophilicity of the membranes. As shown in Figure S4A, the static water contact angle of the membrane decreases dramatically from 95.3 to 81.5°as the OMS content increases from 0 to 3 wt % (Table S3), indicative of the increase of hydrophilicity. It should be attributed to the surface Si-OH groups of the embedded OMS, which is accessible by water through the open macropores in the membrane surface. However, the hydrophilicity of the membrane decreases as the OMS content further increases to 4 and 5 wt % (Figure S5 A). The phenomenon may be related with the lotus-leaf-like surface structures formed when the density of OMS particles is too high, which contribute to the membrane hydrophobicity by increasing surface roughness.[18] Water permeation fluxes of the membranes show the same trend as hydrophilicity, that is, the water permeation flux increases as the OMS content (Figure S5B) increases, and reaches a maximum value (224.5 L m^{-2} h^{-1}) at the OMS content of 3 wt % (Table S2). This phenomenon can be attributed to the following reasons. Due to the hydrophobic nature of PVDF polymers and low porosity (65.0 %) of the pure PVDF membrane, it exhibits the lowest water flux (42.6 L m^{-2} h^{-1}) among the prepared membranes. With the addition of OMS (≤ 3 wt %), water permeation fluxes of the prepared composite membranes are improved due to their higher porosities, 3D interpenetrating porous structures, and more hydrophilic membrane surfaces. On the contrary, the decrease of water fluxes at high OMS contents (> 3 wt %) is attributed to the smaller pore sizes, compacter membrane structures, and the less hydrophilic membrane surfaces caused by the increased surface roughness. Though porosities of the OMS/PVDF-4 and OMS/PVDF-5 are slightly higher than the composite membranes with lower OMS content (Table S2), that contribute little to the improvement of water permeation fluxes. Therefore, the optimal feeding amount of OMS in the casting solution results in OMS/PVDF-3 membranes with the well-developed porous structure, high surface hydrophilicity, and water permeation performance.

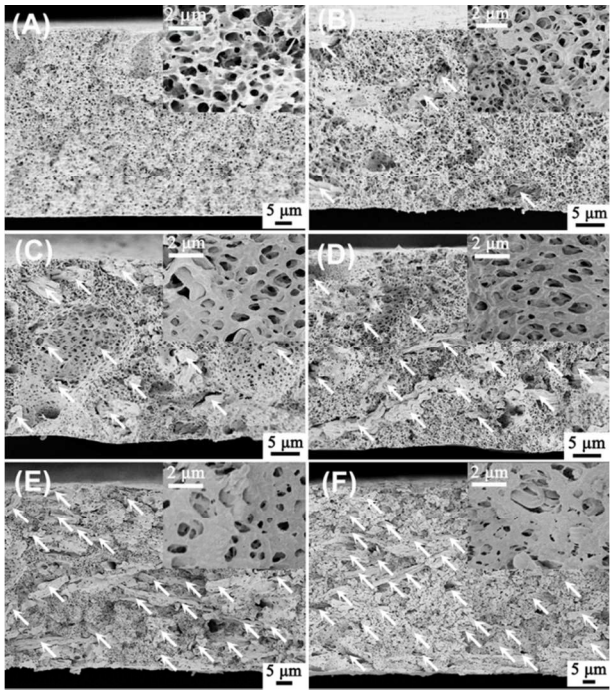

Figure 2. The cross-section SEM images of the membranes with different additions of OMS: A) 0 wt %, B) 1 wt %, C) 2 wt %, D) 3 wt %, E) 4 wt %, and F) 5 wt %. All the weight percentages are based on the weight of the casting solution. OMS particles are marked by white arrows. The insets are the corresponding enlarged images.

N_2 sorption isotherms of the pure PVDF membrane, as well as the OMS/PVDF-3, OMS-NH_2/PVDF-3, and SiO_2/PVDF-3 membranes were further studied (Figure S6). The results show that the OMS/PVDF-3 membrane has the highest surface area (105 m^2 g^{-1}), which is ~ 10 times higher than that of the pure PVDF membrane (Table S3). The embedded mesoporous silica materials dramatically contribute to the total surface areas of the composite membranes.

To understand the influences of the inorganic fillers on water decontamination performances of the membranes, dynamic adsorption tests for methylene blue (MB) by the OMS/PVDF-3 membrane were thoroughly investigated. In the study of the dynamic adsorption of MB, the SiO_2/PVDF-3 membrane and pure PVDF membrane were also tested for comparison. Optical photograph of the device used for the test is shown in Figure 3 A (see supporting information for experimental details). The outlet solution maintained colorless after 200 mL of MB solution (5 mg L^{-1}) were filtrated through the OMS/PVDF-3 membranes, and the effluent concentration was measured to be ~ 0.07 mg/L (Figure 3B-a), suggesting an excellent dynamic adsorption performance. With the increase of permeation volume, the effluent concentration gradually increases, implying that adsorption of the OMS/PVDF-3 membranes gradually approach a saturation value. When the effluent concentration reaches 10% of the feed value, it is normally regarded as the breakthrough point which is adopted to calculate the dynamic adsorption capacity.[21]At the breakthrough point, about 241, 53, and 35 mL of MB solutions have been filtrated through the OMS/PVDF-3 membranes, the SiO_2/PVDF-3 and pure PVDF membranes, respectively (Figure S7A).Thus, the dynamic adsorption capacity for OMS/PVDF-3 membrane is calculated to be 14.5 mg g^{-1}, which is~4.4times higher than that of the SiO_2/PVDF-3 membraneand~9.7 times higher than the pure PVDF membrane (Figure S7A and Table S3). The significant enhancement of dynamic adsorption capacity of the OMS/PVDF-3 membrane can be attributed to three unique features. Firstly, the embedded OMS particles provide a high density of hydrophilic sites for efficiently capturing hydrophilic and basic MB molecules. Secondly, the 3D interpenetrating porous structure of OMS/PVDF-3 membrane facilitates the rapid diffusion of contaminated water, which helps MB molecules interact with the Si–OH groups on the pore walls of OMS. Thirdly, the large pore volume (0.79 cm^{-3} g^{-1}) of the OMS benefits the diffusion of MB molecules (0.4 nm × 0.61 nm × 1.43 nm) into its large mesopores.[22]All the above factors lead to the promising decontamination performance of the OMS/PVDF-3 membrane. By contrast, the SiO_2/PVDF-3 membrane shows low dynamic adsorption capacity due to the nonporous structure and low surface area of the SiO_2 particles. In addition, the pure PVDF membrane exhibits extremely poor affinity for MB molecules due to the lack of active adsorption sites in the PVDF networks, further demonstrating the contribution of OMS to the decontamination performance of the OMS/PVDF-3 membrane.

The regeneration stability of the OMS/PVDF-3 membrane was investigated through a continuous adsorption/desorption test by using a mixed solution of hydrochloric acid (0.5 mg L^{-1})and ethanol

(1/1 by volume) as the eluent (see supporting Information for experimental details). With the permeation of the eluent, the effluent

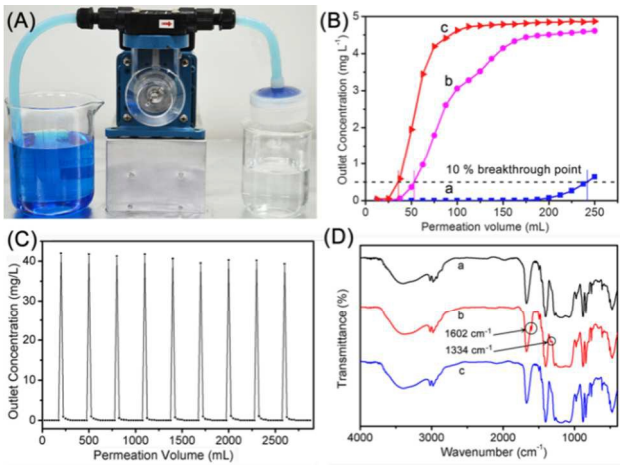

Figure 3.A) The optical photograph of the device for the dynamic adsorption/desorption tests. B) The breakthrough curves for MB solutions by the OMS/PVDF-3 membrane (a), the SiO_2/PVDF-3membrane (b), and the pure PVDF membrane (c). C) Adsorption and desorption of MB by the OMS/PVDF-3 membrane for nine recycling times using a mixture solution of hydrochloric acid (0.5 mg L^{-1}) and ethanol (1/1 by volume) as the eluent. D) FT-IR spectra of the OMS/PVDF-3 membrane before (a) and after (b) the adsorption tests and after regeneration by the eluent (c). All the adsorption tests were carried out with a feed concentration of 5.0 mg L^{-1}.

concentration of MB sharply increases at first and then gradually decreases to undetectable values at the eluent volume of 100 mL (Figure 3C), implying that MB molecules adsorbed on the membranes can be easily eluted. FT-IR spectra of the OMS/PVDF-3 membranes show that two bands at ~1602 and 1334 cm^{-1} attributed to C=N and C-N stretching appear after the adsorption test (Figure 3D-a, b), and then completely disappear after regeneration by the eluent, confirming the total removal of MB molecules from the OMS/PVDF-3 membranes. Moreover, after nine cycles of consecutive regeneration and reuse, the OMS/PVDF-3 membrane almost remains the original adsorption performance (Figure 3C), indicating that the membrane is efficient and stable for the adsorptive removal of MB molecules from aqueous streams. These results imply that the uptake of MB molecules is mainly a physical adsorption process, which is suitable for large scale application in waste water treatment in industry. In addition, ethonal in the eluent can be recovered by distillation and reused in the next adsorption/desorption cycle. Moreover, MB molecules enriched in the eluent can be centralized removed by the oxidative decomposition method.

Amino-group functionalized OMS was used as the filler to prepare composite membranes to demonstrate the versatility of the membrane fabrication process and the applicability for the removal of heavy metal ions. Dynamic adsorption tests for Cu(II) ions by the OMS-NH_2/PVDF-3 membrane with the OMS/PVDF-3 membrane as control were studied. For the OMS-NH_2/PVDF-3 membrane, its dynamic adsorption capacity for Cu(II) ions at breakthrough point is calculated to be 1.5 mg g^{-1} (Figure S7 B and Table S3). However, the effluent concentration of Cu(II) ions for OMS/PVDF-3 membrane at the first 5 min (~ 1.6 mg L^{-1}) is far more beyond the value of 10 % breakthrough point (Figure 4 A-b),suggesting a poor affinity for Cu(II) ions. The phenomenon should be attributed to the lack of active adsorption sites for Cu(II) ions in OMS/PVDF-3 membrane. Whereas, for OMS-NH_2/PVDF-3 membrane, rich –NH_2 groups exist on the pore surface of the embedded OMS-NH_2, which can effectively capture Cu(II) ions by forming the complexes.[23] Therefore, amino-group functionalized OMS endows the obtained membrane with active adsorption sites for Cu(II) ions. In addition, the contrast of the high adsorption capacity for MB by the OMS/PVDF-3 membrane and its poor affinity for Cu(II) ions further confirms that mesoporous fillers with different functional groups can endow the membranes with corresponding active adsorption sites for specific contaminations.

The ethylenediaminetetraacetic acid (EDTA) disodium salt solution (0.5 mg L^{-1}) was used to regenerate the OMS-NH_2/PVDF-3 membrane (see Supporting Information for experimental details). It is observed that the removal rate of Cu(II) ions at a permeation volume of 50 mL slightly declines with increasing regeneration time of the OMS-NH_2/PVDF-3 membrane, but still remains at 90.2 % after recycling for 5 times(Figure 4B). It suggests a good regeneration stability of the OMS-NH_2/PVDF-3 membrane by using EDTA disodium saltsolution as the eluent.

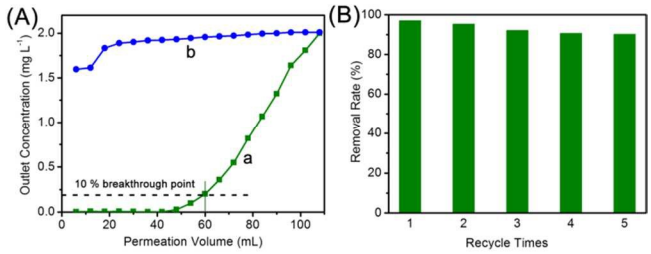

Figure 4.A) The breakthrough curves for Cu(II) ionsby the OMS-NH_2/PVDF-3 (a) and the OMS/PVDF-3 membrane (b), with a flow rate at 39.4 L m^{-2} h^{-1}. B) Removal rates of Cu(II) ions after 50 mL of the feed solution passing through the OMS-NH_2/PVDF-3 membranesas a function of recycle time by using EDTA solution (0.5 mg L^{-1}) as the eluent. All filtration tests were carried out with a feed concentration of 2 mg L^{-1}.

Conclusions

In summary, a versatile and industrially compatible one-step immersion co-precipitation method has been demonstrated for the mass production of mesoporous silica/organic polymer composite membranes headed for efficient dynamic adsorption-removal in water decontamination treatment. The obtained OMS/PVDF composite membranes display good hydrophilicity, high water fluxing ability (224.5 L m^{-2} h^{-1}) and high adsorption capacity (14.5 mg g^{-1}) for methylene blue. The outstanding performance is mainly attributed to 3D interpenetrating porous structure, large pore volume, and abundant Si-OH groups situated on the pore surface of OMS. Simply, by tuning the surface properties of the mesoporous silica filler, amine groups functionalized composite membrane (OMS-NH2/PVDF-3) has been fabricated, which exhibits high adsorption capacity (1.5 mg g^{-1}) for Cu (II) ions towards Cu(II) ions via efficient complexation. More importantly, the composite membranes have high stability for regeneration and reutilization. It is expected that the OMS/PVDF composite membranes possess a great potential for practical applications in the decontamination of aqueous streams containing low-concentration of contaminants. Meanwhile, the entire synthetic approach can

also be extended to design specific composite membranes for waste-gas treatment.

Acknowledgements

This work was supported by the State Key 973 Program of PRC (2013CB934104), the NSF of China (51372041 and 51422202), the "Shu Guang" Project (13SG02), State Key Laboratory of Pollution Control and Resource Reuse Foundation (PCRRF14017), State Key Laboratory of ASIC & System (2015KF002), Qatar University startup grant # QUSG-CAS-MST-14\15-1. the Deanship of Scientific Research at King Saud University for funding the work through the research group project No RGP-227, China Postdoctoral Science Foundation (2014M551455), STCSM (15ZR1402000) Shanghai scientific research plan project (14R21411300), economic and information committee cooperation plan of Shanghai (04002530571), and science and technology committee plan of Shanghai Qingpu district (04002370168).

Notes and references

[a] College of Environmental Science and Engineering, Tongji University, and State Key Laboratory of Pollution Control and Resource Reuse, Shanghai 200092, China

[b] Department of Chemistry and Shanghai Key Laboratory of Molecular Catalysis and Innovative Materials, State Key Laboratory of Molecular Engineering of Polymers, Fudan University, Shanghai 200433, China

[c] State Key Lab of Transducer Technology, Shanghai Institute of Microsystem and Information Technology, Chinese Academy of Sciences, Shanghai 200050, China.

[d] College of Arts and Sciences, Qatar University, PO Box 2713, Doha, Qatar.

[e] Department of Chemistry, College of Science, King Saud University, Riyadh 11451, Saudi Arabia Materials Science and Technology Program.

†Electronic Supplementary Information (ESI) available: See DOI: 10.1039/b000000x/

1 a) Z. X. Wu, D. Y. Zhao, *Chem. Commun*. 2011, **47**, 3332-3338; b) M. Hartmann, *Chem. Mater.* 2005, **17**, 4577–4593; c) J. Wei, Y. Liu, J. Chen, Y. H. Li, Q. Yue, G. X. Pan, Y. L. Yu, Y. H. Deng, D. Y. Zhao, *Adv. Mater.* 2014, **26**, 1782–1787; d) W. Li, Q. Yue, Y. H. Deng, D. Y. Zhao, *Adv. Mater*. 2013, **25**, 5129–5152; e) X. H. Guo, Y. H. Deng, B. Tu, D. Y. Zhao *Langmuir* 2010, **26**,702–708; f) Y. M. Zhang, Z. A. Qiao, Y. T. Li, Y. L. Liu, Q. S. Huo, *J. Mater. Chem*. 2011, **21**, 17283–17289.

2 D. Bruhwiler, *Nanoscale* 2010, **2**, 887-892.

3 Y. Z. Liu, Z. X. Wu, X. Chen, Z. Z. Shao, H. T. Wang, D. Y. Zhao, *J. Mater. Chem*. 2012, **22**, 11908–11911.

4 a) C. F. Xue, B. Tu, D. Y. Zhao, *Adv. Funct. Mater.* 2008, **18**, 3914–3921; b) H. F. Yang, Q. H. Shi, B. Z. Tian, S. H. Xie, F. Q. Zhang, Y. Yan, B. Tu, D. Y. Zhao, *Chem. Mater.* 2003, **15**, 536–541; c) D. Y. Zhao, P. D. Yang, N. Melosh, J. L. Feng, B. F. Chmelka, G. D. Stucky, *Adv. Mater.* 1998, **10**, 1380–1385.

5 a) W. Teng, Z. X. Wu, D. Feng, J. W. Fan, J. X. Wang, H. Wei, M. J. Song, D. Y. Zhao, *Environ. Sci. Technol.* 2013, **47**, 8633-8641; b) J. P. Yang, W. Y. Chen, D. K. Shen, Y. Wei, X. Q. Ran, W. Teng, J. W. Fan, W. X. Zhang, D. Y. Zhao, *J. Mater. Chem. A* 2014, **2**, 11045-11048.

6 a) J. W. Fan, X. Jiang, H. Y. Min, D. D. Li, X. Q. Ran, L. Y. Zou, Y. Sun, W. Li, J. P. Yang, W. Teng, G. M. Li, D. Y. Zhao, *J. Mater. Chem. A* 2014, **2**, 10654-10661; b) A. I. Carrillo, E. Serrano, J. C. Serrano-Ruiz, R. Luque, J. Garcia-Martinez, *Appl. Catal. A-Gen.* 2012, **435**, 1-9; c) C. Wang, J. C. Chen, X. R. Zhou, W. Li, Y. Liu, Q. Yue, Z. T. Xue, Y. H. Li, Y. H. Deng, D. Y. Zhao, *Nano Res.* 2015, **8**, 238-245; d)X. Zhong, J. Barbier, D. Duprez, H. Zhang, S. Royer, *Appl. Catal. B-Envir.* 2012, **121**, 123-134.

7 a) P. Vandezande, L. E. M. Gevers, I. F. J. Vankelecom, Chem. Soc. Rev. 2008, **37**, 365-405; b) M. M. Pendergast, E. M. V. Hoek, *Energy Environmental Sci.*2011, **4**, 1946-1971.

8 a) F. Liu, N. A. Hashim, Y. T. Liu, M. R. M. Abed, K. Li, J. Membr. Sci. 2011, 375, 1-27; b) G. D. Kang, Y. M. Cao, *J. Membr. Sci.* 2014, **463**, 145-165.

9 a) S. P. Roux, E. P. Jacobs, A. J. van Reenen, C. Morkel, M. Meincken, J. Membr. Sci. 2006, **276**, 8-15; b) M. K. Sinha, M. K. Purkait, *J. Membr. Sci.* 2013, **437**, 7-16.

10 a) T. Zhou, Y. Y. Yao, R. L. Xiang, Y. R. Wu, J. Membr. Sci. 2014, **453**, 402-408; b) C. Y. Tu, Y. L. Liu, M. T. Luo, K. R. Lee, J. Y. Lai, *Chemphyschem* 2006, **7**, 1355-1360.

11 H. Uehara, M. Kakiage, M. Sekiya, D. Sakuma, T. Yamonobe, N. Takano, A. Barraud, E. Meurville, P. Ryser, *Acs Nano* 2009, **3**, 924-932.

12 a) S. R. Chae, H. Yamamura, K. Ikeda, Y. Watanabe, Water Res. 2008, 42, 2029-2042; b) J. F. Hester, A. M. Mayes, *J. Membr. Sci.* 2002, **202**, 119-135.

13 a) N. A. Hashim, F. Liu, K. Li, *J. Membr. Sci.* 2009, **345**, 134-141; b) X. Y. Wang, L. Zhang, D. H. Sun, Q. F. An, H. L. Chen, *Desalination* 2009, **236**, 170-178.

14 L. Yan, Y. S. Li, C. B. Xiang, S. Xianda, *J. Membr. Sci*. 2006, **276**, 162-167.

15S. J. Oh, N. Kim, Y. T. Lee, *J. Membr. Sci.* 2009, **345**, 13-20.

16 X. T. Zuo, S. L. Yu, X. Xu, J. Xu, R. L. Bao, X. J. Yan, *J. Membr. Sci.* 2009, **340**, 206-213.

17 a) D. Y. Zhao, Q. S. Huo, J. L. Feng, B. F. Chmelka, G. D. Stucky, *J. Am. Chem. Soc.* 1998, **120**, 6024-6036; b) D. Y. Zhao, J. L. Feng, Q. S. Huo, N. Melosh, G. H. Fredrickson, B. F. Chmelka, G. D. Stucky, *Science* 1998, **279**, 548-552.

18 K. Y. Ho, G. McKay, K. L. Yeung, *Langmuir* 2003, **19**, 3019-3024.

19 M. J. Han, S. T. Nam, *J. Membr. Sci.* 2002, **202**, 55-61.

20 a) L. Jiang, Y. Zhao, J. Zhai, Angew. Chem. Int. Ed. 2004, **43**, 4338-4341; b) X. M. Li, T. He, M. Crego-Calama, D. N. Reinhoudt, *Langmuir* 2008, **24**, 8008-8012.

21 R. Ghosh, T. Wong, *J. Membr. Sci.* 2006, **281**, 532-540.

22 C. Pelekani, V. L. Snoeyink, *Carbon* 2000, **38**, 1423-1436.

23 K. F. Lam, K. L. Yeung, G. McKay, *Langmuir* 2006, **22**, 9632-9641

Entry for the Table of Contents

ARTICLE

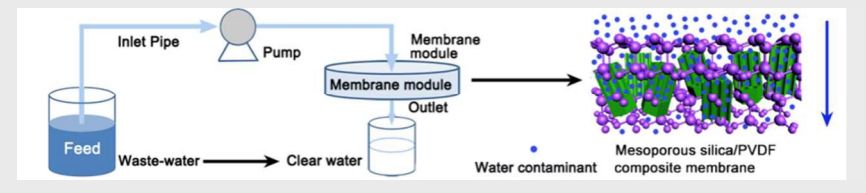

Ordered mesoporous silica/polyvinylidene fluoride (OMS/PVDF) membranes and amino-group functionalized composite membranes (OMS-NH_2/PVDF) with three-dimensional interpenetrating porous structures were fabricated via a versatile and industrially compatible one-step immersion co-precipitation method. They exhibit effective decontamination performance for water containing methylene blue and Cu(II) ions, respectively.

*J. W. Fan, D. D. Li, W. Teng, J. P. Yang, Y. Liu, L. L. Liu,A. A.Elzatahry, A.Alghamdi, Y. H. Deng,*G. M. Li, W.-xian Zhang, D. Y. Zhao**

OrderedMesoporous Silica/Polyvinylidene Fluoride Composite Membranes with Three-Dimensional Interpenetrating Structures for Effective Removal of Water Contaminants